

Characterization of SLC26A9, Facilitation of Cl⁻ Transport by Bicarbonate

Celine Lorient*, Sandrine Dulong*, Martine Avella, Nicole Gabillat, Kim Boulukos, Franck Borgese and Jordi Ehrenfeld

From the Laboratoire de Biologie et Physiopathologie des Systèmes Intégrés, Université de Nice-Sophia Antipolis, CNRS, Nice, *Both first authors (C. Lorient and S. Dulong) have contributed equally to this work

Key Words

Cl⁻ channel • Bicarbonate • Bronchial cells • SLC26 • CFTR

Abstract

SLC26 family members are anionic transporters involved in Cl⁻ and HCO₃⁻ absorption or secretion in epithelia. SLC26A9, preferentially expressed in the lung, is a poorly characterized member of this family. In this study, we investigated the transport properties of human SLC26A9 to determine its functional and pharmacological characteristics. SLC26A9 protein expression results in the appearance of an anionic current exhibiting an apparently linear current/voltage relationship and increases in ³⁶Cl influxes and effluxes. The sequences of conductivity, Cl⁻ > I⁻ > NO₃⁻ ≥ gluconate > SO₄²⁻ and selectivity (P_x/P_{Cl}), I⁻ > NO₃⁻ > Cl⁻ > gluconate > SO₄²⁻ are found. Cl⁻ channel inhibitors DIDS and NS 3623 inhibit SLC26A9 associated currents while the specific CFTR inhibitor (CFTR(inh)-172) or glybenclamide has little effect. Elevation of intracellular cAMP (a CFTR activator) is also ineffective whereas increasing intracellular calcium blocks the SLC26A9 associated currents.

The HCO₃⁻ conductance mediated by the SLC26A9 protein expression is low and no intracellular pH changes are detectable under conditions favoring a Cl⁻/HCO₃⁻ exchange. However, the presence of HCO₃⁻/CO₂ stimulates the Cl⁻-transporting activity of SLC26A9 in *Xenopus laevis* oocytes or SLC26A9-transduced COS-7 cells. As an important initial step in characterizing SLC26A9 function, we conclude that SLC26A9 is a Cl⁻ channel and we suggest that HCO₃⁻ acts as a modulator of the channel. SLC26A9 physiological role in airway epithelia and its potential interaction with CFTR remain to be elucidated.

Copyright © 2008 S. Karger AG, Basel

Introduction

SLC26 proteins are members of a family of anion transporters consisting of 10 known members [1]. Among these anion transporters, most of them are expressed in the luminal membranes of epithelial cells [1] and at least half of them appear to play an important role in epithelial Cl⁻ and HCO₃⁻ transport. For example, SLC26A3 is a

KARGER

Fax +41 61 306 12 34
E-Mail karger@karger.ch
www.karger.com

© 2008 S. Karger AG, Basel
1015-8987/08/0224-0015\$24.50/0

Accessible online at:
www.karger.com/cpb

J. Ehrenfeld
Laboratoire de Biologie et Physiopathologie des Systèmes Intégrés
Université de Nice-Sophia Antipolis, CNRS, FRE 3094
Parc Valrose, 28 avenue Valrose, 06108 Nice Cedex 2 (France)
Tel. +33492076836, Fax +33492076834, E-Mail Jordi.EHRENFELD@unice.fr

coupled $\text{Cl}^-/\text{HCO}_3^-$ exchanger [2, 3] predominantly expressed in the digestive system [4]. SLC26A4 functions as an anion exchanger in the kidney [5] but also as an iodide transporter in the thyroid or kidney [2, 6-8]. SLC26A6 is a versatile anion exchanger functioning as a coupled $\text{Cl}^-/\text{HCO}_3^-$ exchanger but also as an exchanger for $\text{Cl}^-/\text{oxalate}$, $\text{SO}_4^{2-}/\text{oxalate}$, $\text{Cl}^-/\text{formate}$ and Cl^-/OH^- when expressed in *Xenopus laevis* oocytes [1, 9]. SLC26A7, -A8 and -A9 are expressed in human kidney, testis and lung, respectively [10]. SLC26A9 was initially identified in gastric epithelia where it was proposed to mediate a $\text{Cl}^-/\text{HCO}_3^-$ exchange [11]. However, it was recently found to function as a Cl^- channel regulated by WNK kinases [12]. Interestingly, SLC26A7, another SLC26 transporter, present in gastric parietal cells and in intercalated cells of the outer medullary collecting tubule, initially reported to function as an anion exchanger [13] was more recently characterized as a Cl^- channel regulated by intracellular pH [14].

CFTR plays a major role in Cl^- transport in airway tissue but other chloride channels have been described to participate to transepithelial Cl^- transport. ORCC (outward rectified chloride channel), CaCC (Calcium-activated chloride channel) or ClC-2 are examples of proposed and potential “alternative CFTR Cl^- channels” [15-19]. Mutual interactions exist between CFTR and these reported Cl^- channels, yet the precise mechanisms of interaction remain unclear [20-24].

A reciprocal regulation between the CFTR chloride channel, implicated in cystic fibrosis and several members of the SLC26 family has been described [2]. In their study, activation of CFTR by SLC26A3 (DRA) and SLC26A6 was facilitated by their PDZ ligands and binding of the STAS domains of SLC26 transporters to the CFTR R domain.

As an approach to understand the role of human SLC26A9 in airway epithelia, we first wished to define its functional characteristics using two different protein expression systems: *Xenopus laevis* oocytes and retrovirally transduced COS-7 cells. SLC26A9 transport properties were established by measuring its anion selectivity, pharmacological sensibility and sensitivity to cAMP and Ca^{2+} , two intracellular mediators regulating ion transport in epithelia. We find that SLC26A9 behaves as a Cl^- channel and not as an anion exchanger, presenting in addition a very low HCO_3^- permeability. However, we demonstrate that the presence of $\text{HCO}_3^-/\text{CO}_2$ by itself stimulates the Cl^- transport mediated by SLC26A9 and could act as a positive regulator by a direct interaction with the channel.

Material and Methods

Cloning of the full length SLC26A9

Primary cultures of bronchial cells (NHBE, Cambrex, East Rutherford, NJ) were grown on inserts (Transwell-Clear, Corning Inc, NY, USA), then exposed to an apical air interface for two weeks (details of medium and culture conditions were performed according to Cambrex corporation). Total RNA was prepared from NHBE cells according the protocol of Chomczynski and Sacchi [25]. mRNA was then purified by affinity chromatography on oligo(dT)-cellulose and reverse transcribed using “SuperScript™ First-Strand Synthesis System for RT-PCR” kit from Invitrogen (Carlsbad, CA). A nested primer PCR strategy was used to amplify SLC26A9 cDNA using oligonucleotides derived from the human SLC26A9 sequence AF331525 (NCBI). The first PCR was performed using primers SLC26A9up1, 5'-gag cag agc cct ttc aca cac ctc-3', and SLC26A9dw1, 5'-acc aag gcc tag act cct ggg-3'. The nested PCR was done with the oligonucleotide couple: SLC26A9up, 5'-aca cct ttc ggc tgc ccg ctc c-3' and SLC26A9dw, 5'- gag gaa ccc aag ctc tgg ggg-3'. PCR product was purified, then ligated into the pGEMT-easy vector (Promega, Madison, WI). The SLC26A9 cDNA was then subcloned into the plasmid pSP64poly(A) (Promega) downstream of the SP6 RNA promoter. A positive clone was independently sequenced twice using a set of seven oligonucleotides to verify the integrity of the sequence. cRNA was produced using the mMESSAGE mMACHINE SP6 following the manufacture's guidelines (Ambion, Countaboeuf, France).

SLC26A9-transduced COS-7

The coding sequence of SLC26A9 was excised from pSP64 by using *XhoI* and *SstII* restriction enzymes, then analyzed by agarose gel electrophoresis. After gel extraction and purification (NucleoSpin ExtractII, Macherey-Nagel, Hoerd, France), the SLC26A9 cDNA fragment was subcloned into the *XhoI* and *SacII* restriction sites of the mammalian expression vector pPRIG-eGFP [26] to generate pPRIG-eGFP-SLC26A9. Highly pure recombinant plasmids were obtained by anion-exchange chromatography (NucleobondAx, Macherey-Nagel) and were used to stably transduce COS-7 cells. Similarly, SLC26A9 was subcloned in pPRIG-HA-eGFP vector. SLC26A9 was ligated in-phase downstream of the HA tag epitope to generate a tagged HA-protein (tag added at the N-terminal part of the protein). The construct was used to transduce HEK cells. For transduction experiments, HEK293 cells were seeded at 30-40% density in 60 mm dishes in DMEM supplemented with 10 % FCS. To generate retroviruses, 293T cells were transfected the following day with 2.5 μg of an empty pPRIG-eGFP plasmid or the pPRIG-eGFP-SLC26A9 construct, and with 1.25 μg of pCMV-VSVG and 1.25 μg of pCMV-gag-pol plasmids using the classic calcium phosphate transfection technique. 6 h post-transfection, cells were washed and fresh medium was added. Replication-defective retroviruses were recovered in the culture medium between 24 h and 72 h post-transfection. These retroviral supernatants were filtered through sterile 0.45 μm filters, then added directly to COS-7 cells in the presence of 4 $\mu\text{g}/\text{ml}$ polybrene to enhance retroviral transduction efficiency.

Mixed populations of control (empty vector) or SLC26A9 expressing COS-7 cells were obtained due to independent integrations of the retroviruses into the host COS-7 cell genome. eGFP-positive transduced cells were observed as early as 24 h post transduction. Over 95% of the cells were efficiently transduced. Western analyses were performed as described below for oocytes. The HA-tagged SLC26A9 protein was detected using an anti-HA antibody in HEK-293 cells.

*Functional expression in *Xenopus laevis* oocytes and voltage-clamp analysis*

cRNAs (15 ng cRNA per oocyte, unless otherwise indicated) were injected into collagenase-defolliculated oocytes from *Xenopus laevis*, prepared and handled as previously described [27, 28]. Oocytes were maintained at 18°C in MBS (Modified Barth's Saline) containing (in mM): 85 NaCl, 1 KCl, 2.4 NaHCO₃, 0.82 MgSO₄, 0.33 Ca(NO₃)₂, 0.41 CaCl₂, 10 HEPES (N-2-hydroxyethyl)piperazine-N'-(2-ethanesulfonic acid), 3 NaOH, pH 7.4, supplemented with penicillin (6 mg/l) and streptomycin (10 mg/l).

Two-electrode voltage-clamp measurements were performed at room temperature in MBS (in the absence of antibiotics) as previously described [28] or in different anion or cation substituted media (see below for composition). Briefly, oocytes were voltage-clamped at a holding potential of -30 mV and 800 ms voltage steps from -100 mV to +80 mV in 20 mV increments were applied using a TEV 200 amplifier (Dagan, Minneapolis, MN) and monitored by computer through Digidata 1200A/D converter and pCLAMP 6.0 software (Axon Instruments, Foster City, CA). In other experiments, currents were followed as a function of time at a constant clamping voltage. All data are presented as mean values \pm standard error (n = number of observations). The Student's t-test was used for all statistical analyses.

Western blotting

Oocytes were homogenized in homogenization buffer (250 mM Sucrose, 0.5 mM ethylenediaminetetraacetic acid (EDTA), 5 mM Tris-HCl, pH 7.4) supplemented with the protease inhibitor cocktail "Complete" (Roche Molecular Biochemicals, Mannheim, Germany) then centrifuged three times for 15 min at 2,000 rpm, 4,000 rpm and 6,000 rpm in a refrigerated (4°C) Heraeus centrifuge. Supernatants were then centrifuged at 65,000 rpm for 45 min in an ultracentrifuge at 4°C (Sorvall Discovery M150, France) and the pellets were suspended in RIPA (NaCl 150 mM, Triton 100X 1%, DOC 0.5%, SDS 0.1%, TRIS pH 8.0, PMSF 1 mM). 70 μ g of protein were loaded per lane. After addition of reducing Laemmli sample buffer (LSB) to the cleared supernatants, proteins were denatured, separated by 7.5% SDS-polyacrylamide gel electrophoresis and electrotransferred onto nitrocellulose membranes (Hybond C-Extra, Amersham, Orsay, France). Nonspecific protein absorption was prevented by incubating the membranes (1 h) in Tris-buffered saline containing Tween-20 (TBS-T) and BSA (3%). Primary incubation was performed overnight at 4°C in TBS-T containing BSA with a rabbit polyclonal antibody directed against 16 C-terminal amino acids of SLC26A9 (lydseedirsywdleq) at a final dilution of 1:500. The (HRP)-couple anti-rabbit secondary antibody was

used at a final dilution of 1:5000. HRP was revealed by a chemiluminescent detection system (Supersignal, Pierce Biotechnologie, Brebieres, France). Anti HA (clone HA7, Sigma) was used at a final dilution 1/1000. Anti-mouse peroxidase conjugate (Sigma) was used at a final dilution 1/40 000.

Measurement of intracellular pH (pH_i) in oocytes

For pH_i measurements, borosilicate-silanized microelectrodes were prepared as described previously [29]. Briefly, a small drop (0.3 μ l) of proton exchanger resin (Hydrogen ionophore I-cocktail A: ref Fluka 95291) was introduced into the tip of the microelectrodes, back-filled with phosphate buffer (pH 7.0) and calibrated in pH solutions at pH 6.8 and 8.0. The electrode was fitted with a holder with an Ag-AgCl wire attached to a high impedance probe of a two channel FD-223 electrometer (Word Precision Instruments, Sarasota, Florida, USA). A standard electrode filled with 3M KCl was connected to the other channel of the electrometer for the measurement of membrane potential measurements. The bath was grounded via a 3M KCl agar bridge connected to an Ag-AgCl wire. The signal from the voltage microelectrode was subtracted from the pH electrode to obtain the pH_i changes. The slope of the pH electrodes was between 54 mV and 58 mV per pH unit.

Measurement of Cl_i and pH_i in COS-7 cells

For measurements of Cl_i and pH_i , cells grown on filters were cut off the Transwell and mounted into a modified Ussing chamber as previously described [30]. The fluorescence was measured with a spectrophotometer system (PTI Deltascan, N.J., USA). MQAE (Molecular probes, Eugene Ore, USA) was used as a probe of cellular Cl^- , at a loading concentration of 8 mM (overnight in a CO₂ incubator). For MQAE measurements, excitation was set at 350 nm and emission was monitored at 450 nm. The fluorescence intensity was measured every three seconds and plotted graphically. At the end of the experiment, the monolayer was perfused with a KSCN (120 mM) solution (buffered with 10 mM HEPES/KOH, pH 7.2) which quenched MQAE fluorescence by >90%. For data analysis, this value was subtracted from the fluorescence measured experimentally. Results were expressed as a ratio of fluorescence F/F₀, with F₀ being the maximum of fluorescence obtained in absence of chloride (the extra-cellular Cl^- concentration was changed at an equimolar substitution of NO₃⁻ for Cl^-).

Cells were loaded with BCECF/AM (Molecular probes) as a probe of cellular pH, at a loading concentration of 5 μ M for 15-30 min. For BCECF, excitation lights was set at 430 nm and 490 nm at a rate of 100 Hz and emission was monitored at 540 nm (6 nm band pass). A calibration curve was performed at the end of each experiment by application of a 100 mM KCl, 10 mM HEPES solution containing nigericin (5 μ M) and buffered at pH 6.4 or pH 7.8.

³⁶Cl fluxes in oocytes

³⁶Cl influxes (uptake) and ³⁶Cl effluxes were performed in non-injected and SLC26A9 cRNA-injected *Xenopus laevis* oocytes. For ³⁶Cl uptake experiments, oocytes were incubated for 15 min in MBS, washed three times with a cold Cl^- free MBS

and then lysed in MBS containing SDS (final concentration 0.6%). The radioactive samples were counted using a liquid scintillation counter (Packard Instruments, Meriden, CT, USA) after the addition of 4 ml liquid scintillation fluid (ACS, Amersham). The ^{36}Cl uptake is expressed in neq/h/oocyte. For ^{36}Cl efflux experiments, oocytes were first loaded overnight at 18°C and then washed three times in MBS before following ^{36}Cl effluxes during a period of 15 min (each oocyte was bathed in a 500 μl MBS solution). Collected samples and lysed oocytes were then counted for ^{36}Cl radioactivity (see above). Effluxes were expressed as the percentage (%) per min of ^{36}Cl loss into the medium relative to the total ^{36}Cl contained in the oocyte.

Chemicals

Chloride channel inhibitors: DIDS (4,4'-Diisothiocyanatostilbene-2,2'-disulfonic acid, Disodium salt), glybenclamide (N-p-{2-(5-Chloro-2 methoxybenzamido)ethyl}benzenesulfonyl-N'-cyclohexylurea), ionomycin, forskolin, 3-isobutyl-1-methylxanthine (IBMX) and thapsigargin were purchased from Sigma (Sigma Chemical Co., MO, USA). NS 3623 and NS 1652 were a generous gift from P. Christophersen (Copenhagen, DK), CFTR(inh)-172 was a generous gift from A. Verkman (San Francisco, USA).

Results

Functional expression of SLC26A9 in *Xenopus laevis* oocytes

We first assessed the functional expression of SLC26A9 by measuring the Cl^- transport capacity in cRNA-injected oocytes. An increase in the amplitude of Cl^- transport is observed in SLC26A9 cRNA-injected oocytes compared to non-injected oocytes (Fig. 1A). An increase in Cl^- transport capacity is observed when measuring ^{36}Cl effluxes (20 X increase, $p < 0.0001$, $n = 10$) and in ^{36}Cl uptake experiments (21 X increase, $p < 0.0001$, $n = 5$) indicating that SLC26A9 conducts chloride ions. In these experiments performed in open-circuit conditions, the small depolarization of the membrane potential which is observed (see below) in SLC26A9 cRNA-injected oocytes should be taken in consideration. This will slightly over-estimate the ^{36}Cl influxes and under-estimate ^{36}Cl effluxes between both batches of oocytes but will not modify our conclusion that SLC26A9 conducts chloride ions.

In a second set of experiments, we tested whether SLC26A9 expression was associated with the appearance of a new ion conductive pathway. Such a behavior would be expected to be associated with the functioning of an electrogenic carrier or an ion channel. For this purpose, we measured the electrophysiological characteristics of *Xenopus laevis* oocytes expressing SLC26A9. SLC26A9

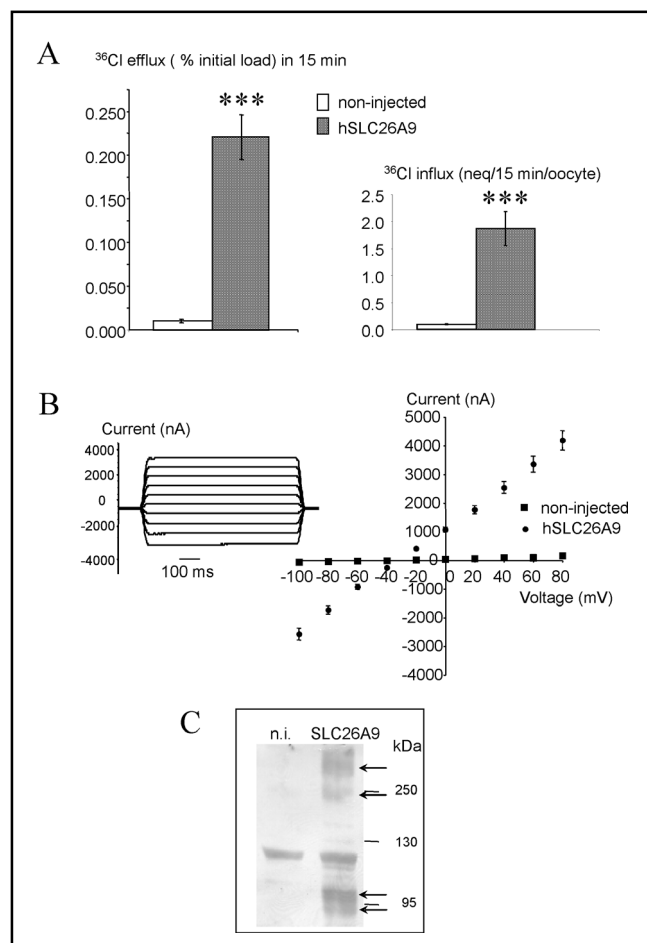


Fig. 1. Functional expression of SLC26A9 in cRNA-injected oocytes. (A) Increases in ^{36}Cl efflux ($n = 10$) and ^{36}Cl uptake ($n = 5$) are observed in SLC26A9 cRNA-injected oocytes compared to non-injected oocytes. (B) Oocytes expressing SLC26A9 display new currents (left panel). The means of the I/V relationships of non-injected oocytes ($n = 13$) and SLC26A9 cRNA-injected oocytes (15 ng/oocyte, $n = 43$) are given in the right panel. Measurements were made 3 to 4 days after RNA injection. *** $P < 0.001$, significant differences between non-injected and SLC26A9 cRNA-injected oocytes. (C) SLC26A9 immunoblot of microsomal membranes from oocytes injected with SLC26A9 cRNA (3 days after injection) and of membranes from non-injected oocytes. New migrating protein products corresponding to predicted monomeric and multimeric SLC26A9 forms are observed only in cRNA-injected oocytes (arrows). The molecular weight markers at 95, 130 and 250 kDa are indicated.

cRNA-injected oocytes present a small but significant ($p < 0.0001$) membrane potential depolarization (-29.8 ± 0.7 mV, $n = 46$) compared to control oocytes (-36.5 ± 1.4 mV, $n = 24$). SLC26A9 cRNA-injected oocytes develop currents not observed in non-injected oocytes (Fig. 1B). Analyses of the current traces of SLC26A9 cRNA-injected oocytes are found to be time-independent and

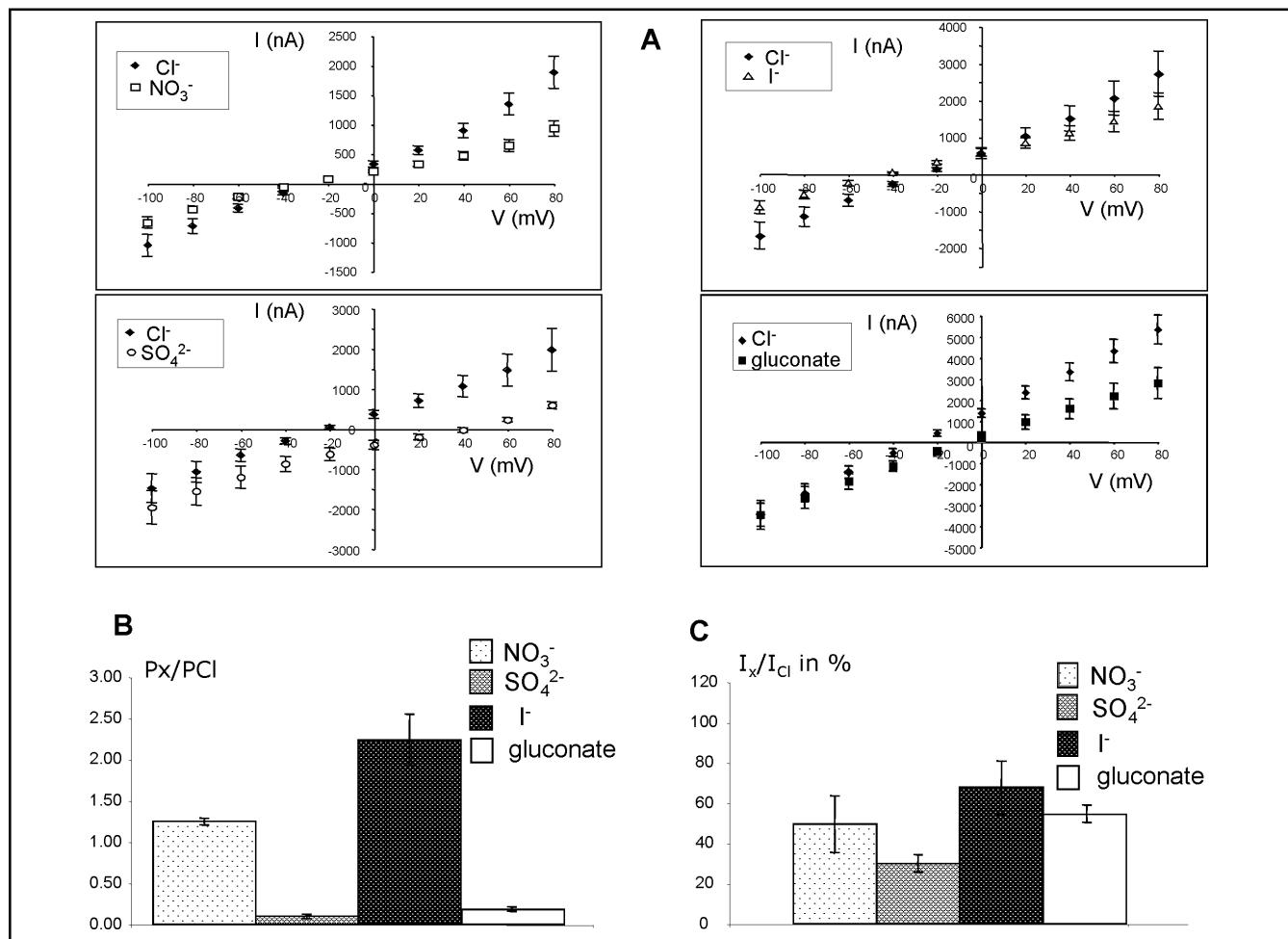


Fig. 2. SLC26A9 anion selectivity. (A) I/V relationships were performed using SLC26A9 cRNA-injected oocytes bathed in MBS (85 mM Cl⁻) and then perfused with a similar medium containing I⁻, NO₃⁻, SO₄²⁻ or gluconate instead of Cl⁻. (B) Maximal potential changes occurring when perfusing from MBS to a Cl⁻-free medium are taken into account to calculate P_x/P_{Cl} . (C) The mean \pm ES of the anion current ratios at +80 mV (in % of Cl⁻ currents) are given. Values represents the mean of 10 oocytes for Cl⁻ to NO₃⁻, 8 for Cl⁻ to SO₄²⁻, 6 for Cl⁻ to I⁻ and 10 for Cl⁻ to gluconate-substitution experiments.

the resulting I/V relationships are found to be apparently linear or slightly outwardly rectified (see Fig. 2) in presence of a membrane Cl⁻ concentration gradient (our experimental conditions).

SLC26A9 protein expression was confirmed by Western blot analysis using microsomal membranes prepared from non-injected oocytes and from SLC26A9 cRNA-injected oocytes. As shown in Fig. 1C, several bands not observed in non-injected oocytes are detected in SLC26A9 cRNA-injected oocytes. One of them migrates slightly lower and another slightly higher than 95 kDa. The lower band corresponds to the monomeric form of SLC26A9 with the expected predicted molecular weight of 87 kDa. Another band is observed around 250 kDa and above. Higher bands could correspond to dimeric or tetrameric forms or even aggregates of SLC26A9. A

non-specific band migrating at approximately 120 kDa is unrelated to SLC26A9 since it is also observed in non-injected oocytes.

SLC26 family members have been reported to transport anions [1, 2, 10]. The value of the reversal potential of the I/V relationship found with SLC26A9 cRNA-injected oocytes which is close to the calculated equilibrium potential of Cl⁻ (assuming a Cl_i of 27 meq/l; unpublished data) points to a dominant Cl⁻ conductance. We assessed the SLC26A9-associated currents to Cl⁻ concentrations of the oocyte perfusing medium in a Cl⁻ concentration ranging from 0 to 80 mM NaCl (Cl⁻ was substituted by gluconate). A linear relationship ($r=0.99$, $n=5$) is found between currents (measured at +80 mV) and Cl⁻ concentrations of the perfusing medium confirming the conductance of SLC26A9 to Cl⁻.

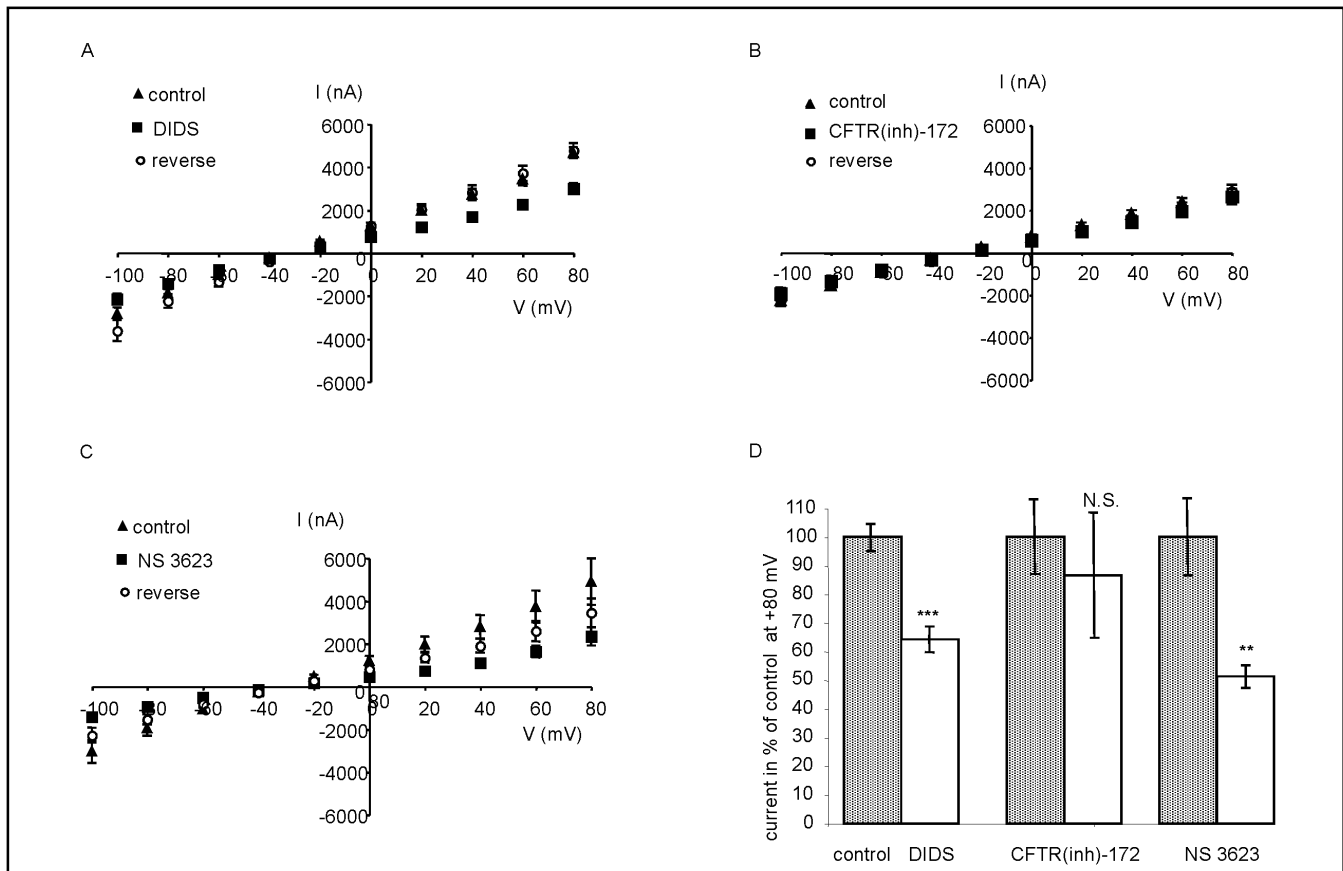


Fig. 3. Effect of some anionic channel or carrier inhibitors on the I/V relationships. (A) Effect of 500 μ M DIDS, n=6 (B) Effect of 2 μ M CFTR(inh)-172, n=9, (C) effect of 500 μ M NS 3623 (n=7). After a control I/V, the drug is tested 2 (data not shown) and 5 min after their application followed by a 10 min reversal period. (D) The mean \pm ES currents measured at +80 mV. Experiments are performed in MBS. *** P < 0.005, ** p < 0.01, significance of the difference of currents with and without inhibitors at +80 mV.

Therefore we assessed the selectivity of SLC26A9 to anions by substituting chloride in I/V experiments (Fig. 2). Measurements of the reversal potentials and calculations of the P_x/P_{Cl} ratio show that SLC26A9 presents a P_x/P_{Cl} ratio (selectivity sequence) of $I^- > NO_3^- > Cl^- > gluconate > SO_4^{2-}$ (Fig. 2B). The sequence of currents measured at +80 mV (outward current) is $Cl^- > I^- > NO_3^- \geq gluconate > SO_4^{2-}$ (Fig. 2C). Furthermore, it can be noticed that the currents in the negative potential range, associated mainly to Cl^- effluxes, are also partly blocked by Cl^- substitution by NO_3^- or I^- . This can be seen at -100 mV, where I is reduced by $33.8 \pm 2.7\%$, n=10, $p < 0.001$ and by $45.8 \pm 5.7\%$, n=6, $p < 0.001$ for Cl^- to NO_3^- and Cl^- to I^- substitutions, respectively. Such an inhibitory effect of NO_3^- and I^- on Cl^- transport has already been reported [12].

We considered the possible development of a cationic (Na^+) pathway associated with SLC26A9 expression by substituting Na^+ by NMDG in the perfusing solution. Such a substitution does not significantly affect the current in

both positive and negative potential ranges (1312 ± 122 nA at 80 mV and -1159 ± 134 nA at -100 mV in MBS versus 1271 ± 128 nA at 80 mV and -1243 ± 175 nA at -100 mV in NMDG-solution, n=12) nor the reversal potential of the I/V relationship (change of 3.0 ± 2.0 mV, N.S.).

Sensitivity of SLC26A9 to some anion inhibitors

We tested some anion channel inhibitors on the I/V relationships of SLC26A9 cRNA-injected oocytes (Fig. 3). DIDS (500 μ M) blocks by $38 \pm 6\%$ ($p < 0.005$, n=6), the SLC26A9-associated currents (measured at +80 mV) after 5 min of application (Fig. 3A and D). Its effect is reversible upon washing. CFTR(inh)-172 (2 μ M) had no significant inhibitory effect (Fig. 3B and D; n=10). As a positive control, CFTR cRNA-injected oocytes were perfused with a forskolin/IBMX (5 μ M/100 μ M)-containing solution. An increase of 6.3 ± 1.5 fold ($p < 0.005$) is observed for currents (value at +80 mV, n=9) following 5 min of the cocktail application. Stimulated currents are

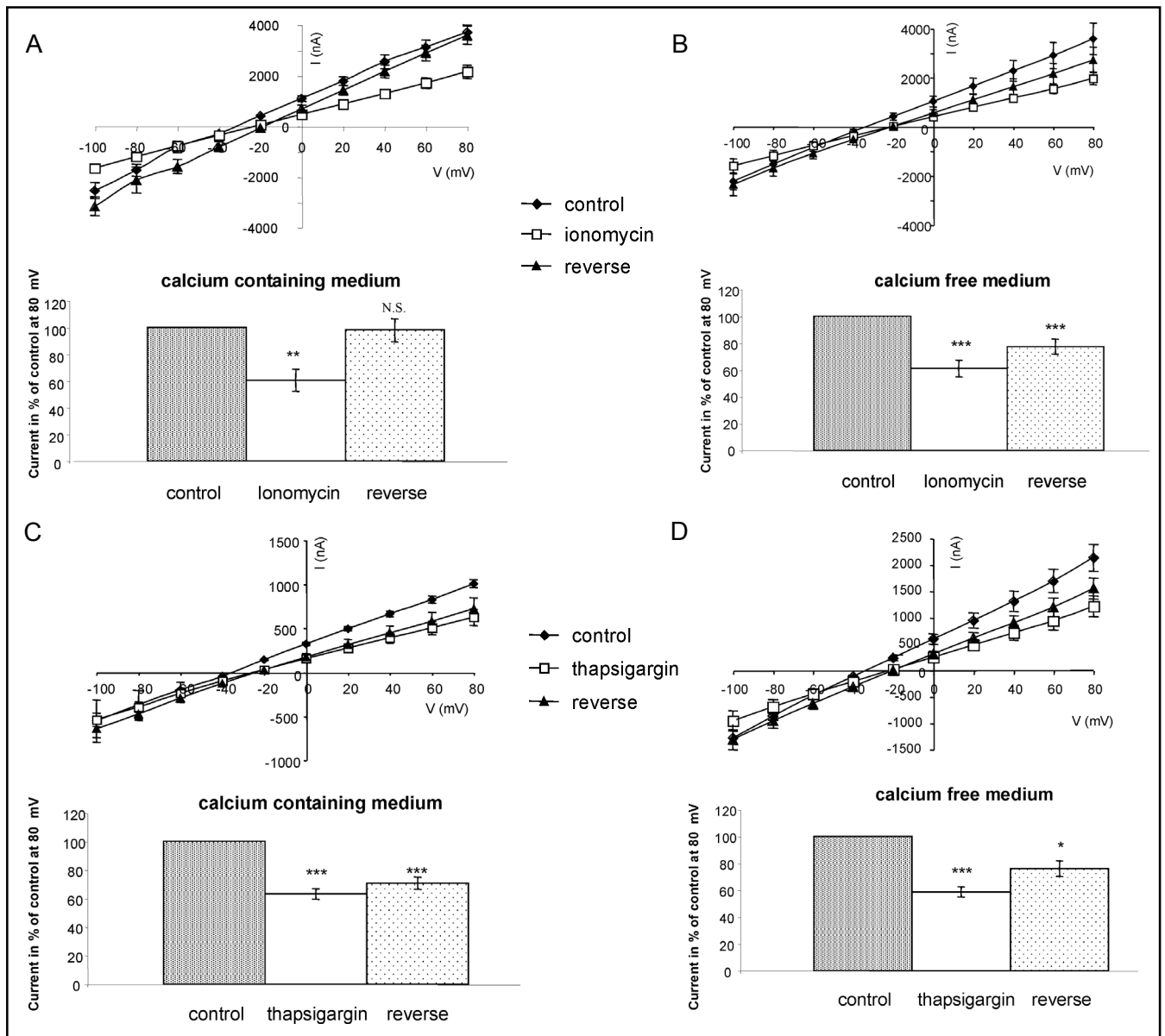


Fig. 4. Intracellular calcium inhibits currents associated to SLC26A9 expression. Effect of ionomycin application on the I/V relationship of SLC26A9 cRNA-injected oocytes (upper part of A and B) and of mean currents (\pm ES) at +80 mV (lower part of A and B) with oocytes bathed in a calcium containing medium (A, $n=11$) or in a calcium free medium containing 100 μ M EGTA (B, $n=10$). Measurements performed at 10 min of ionomycin (0.29 μ M) application and after 10 min of reversal with MBS. Effect of thapsigargin application on the I/V relationship of SLC26A9 cRNA-injected oocytes (upper part of C and D) and of mean currents (\pm ES) at +80 mV (lower part of C and D) with oocytes bathed in a calcium containing medium (C, $n=11$) or in a calcium free medium containing 100 μ M EGTA (D, $n=10$). Measurements performed at 15 min of thapsigargin (400 nM) application and after 10 min of reversal with MBS perfusion. *** $P < 0.005$, ** $p < 0.001$, * $p < 0.01$, significance of the difference of currents with and without tested agents at +80 mV.

further blocked by $40 \pm 6\%$, $n=9$ ($p < 0.0001$) by the CFTR(inh)-172 (2 μ M). Two other blockers of anion channels or carriers [31] were also tested. NS 3623 (500 μ M) blocks $49 \pm 4\%$ of the current ($p < 0.01$, $n=7$) after 5 min of application (Fig. 3C and D) while NS 1652 (500 μ M) has no effect (data not shown).

Inhibitory effect of Ca_i increases on SLC26A9 activity

In order to gain insight on SLC26A9 regulation, we investigated the effect of changing Ca_i on SLC26A9 activity. A transient calcium-activated anion current develops in *Xenopus laevis* oocytes when increasing Ca_i ,

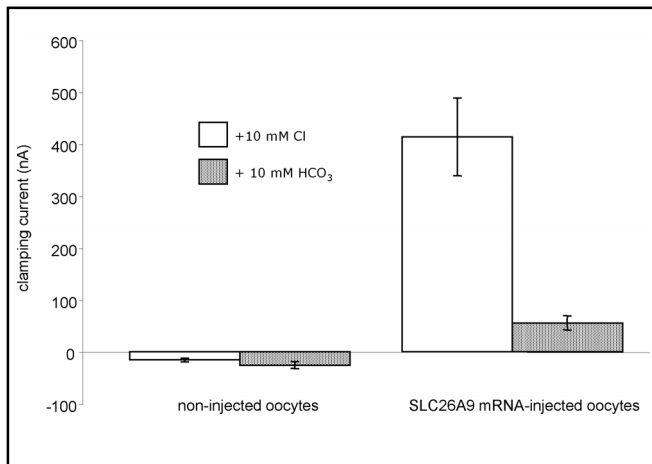


Fig. 5. SLC26A9 cRNA-injected oocytes present a low HCO_3^- conductance compared to Cl^- . Mean \pm ES of the changes in current following passages from a Kgluconate solution to one containing 10 mM Cl^- or 10 mM HCO_3^- ($n=10$). Clamping currents of non-injected oocytes are given as control ($n=8$).

but this current returns to slightly higher amplitudes than initial currents after 5 min [28]. Therefore, in the present experiments, currents were measured after 10 to 15 min of ionomycin (0.25 μM) or thapsigargin (400 nM) application in the presence or absence of calcium in perfusing medium. Non-injected oocytes present low currents over the clamping voltage range used and currents are not significantly affected by ionomycin or thapsigargin application after 10 min of drug administration (data not shown). However, their reversal potential shows a shift similar to that found for SLC26A9-mRNA injected oocytes which could be associated to the opening (and to the almost complete closing after 10 min) of endogenous calcium-activated Cl^- channels. By contrast, ionomycin inhibits the currents associated with SLC26A9 expression in cRNA-injected oocytes (Fig. 4A). This effect is still observed when ionomycin is added in a calcium-free perfusing solution (Fig. 4B). This last finding is consistent with the reported observation in *Xenopus laevis* oocytes that ionomycin has a dual effect, acting on the membrane permeability but also inducing a calcium release from intracellular stores [32]. Washing out (10 min) ionomycin from the perfusing solution partly reverses its inhibitory effect (Fig. 4A and 4B). Thapsigargin, an agent known to liberate calcium from intracellular stores [33], also induces an inhibition of currents in SLC26A9 cRNA-injected oocytes (Fig. 4C and 4D). In contrast to ionomycin experiments, thapsigargin effect is poorly reversible after 10 min of oocyte MBS washing.

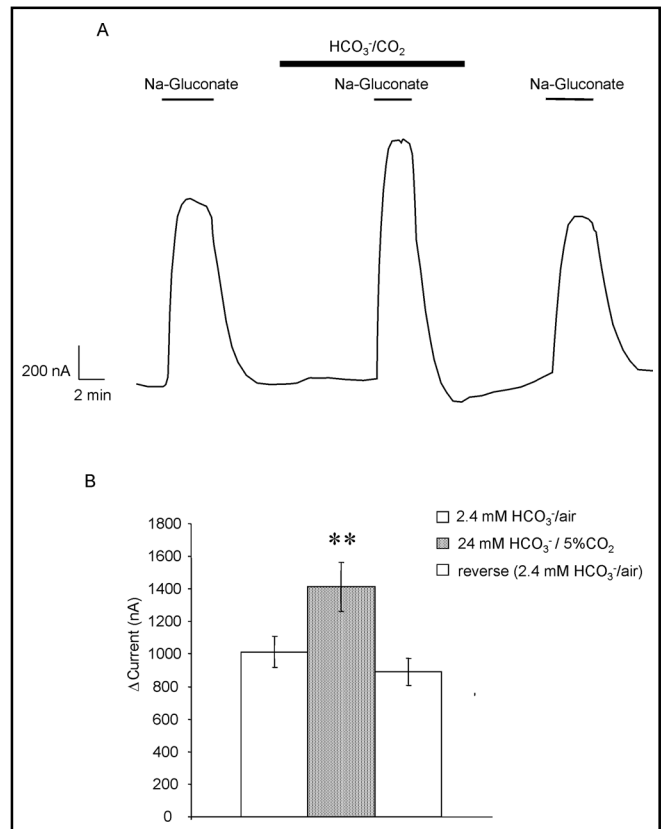


Fig. 6. $\text{HCO}_3^-/\text{CO}_2$ stimulates Cl^- conductance in SLC26A9 cRNA-injected oocytes. (A) Illustrative experiment of the clamping currents measured when the medium perfusing the oocyte is changed from MBS to Cl^- -free medium (Nagluconate). This experiment is performed successively in a 2.4 mM $\text{HCO}_3^-/\text{CO}_2$ -free medium and in a 24 mM $\text{HCO}_3^-/5\%\text{CO}_2$ -containing medium. (B) The mean \pm ES of the clamping currents, $n=12$, $p<0.001$. No significant changes in currents were observed in non-injected oocytes (data not shown).

In order to study a possible regulation of SLC26A9 by an associated cAMP-regulatory pathway, we investigated the effect of cAMP in SLC26A9 cRNA-injected oocytes by increasing cAMP in applying a cocktail of forskolin (5 μM) and IBMX (0.5 mM) for 10 min. No change in currents associated to SLC26A9 protein expression (data not shown, $n=6$) was observed by forskolin/IBMX application.

SLC26A9 is a Cl^- channel weakly permeable to HCO_3^-

In order to compare Cl^- to HCO_3^- permeability of SLC26A9 cRNA-injected oocytes, we measured the current changes following oocyte perfusion from a Kgluconate medium to one supplemented with Cl^- (10 mM) or HCO_3^- (10 mM) (see methods for media composition). Switching from a high Cl^- -containing medium

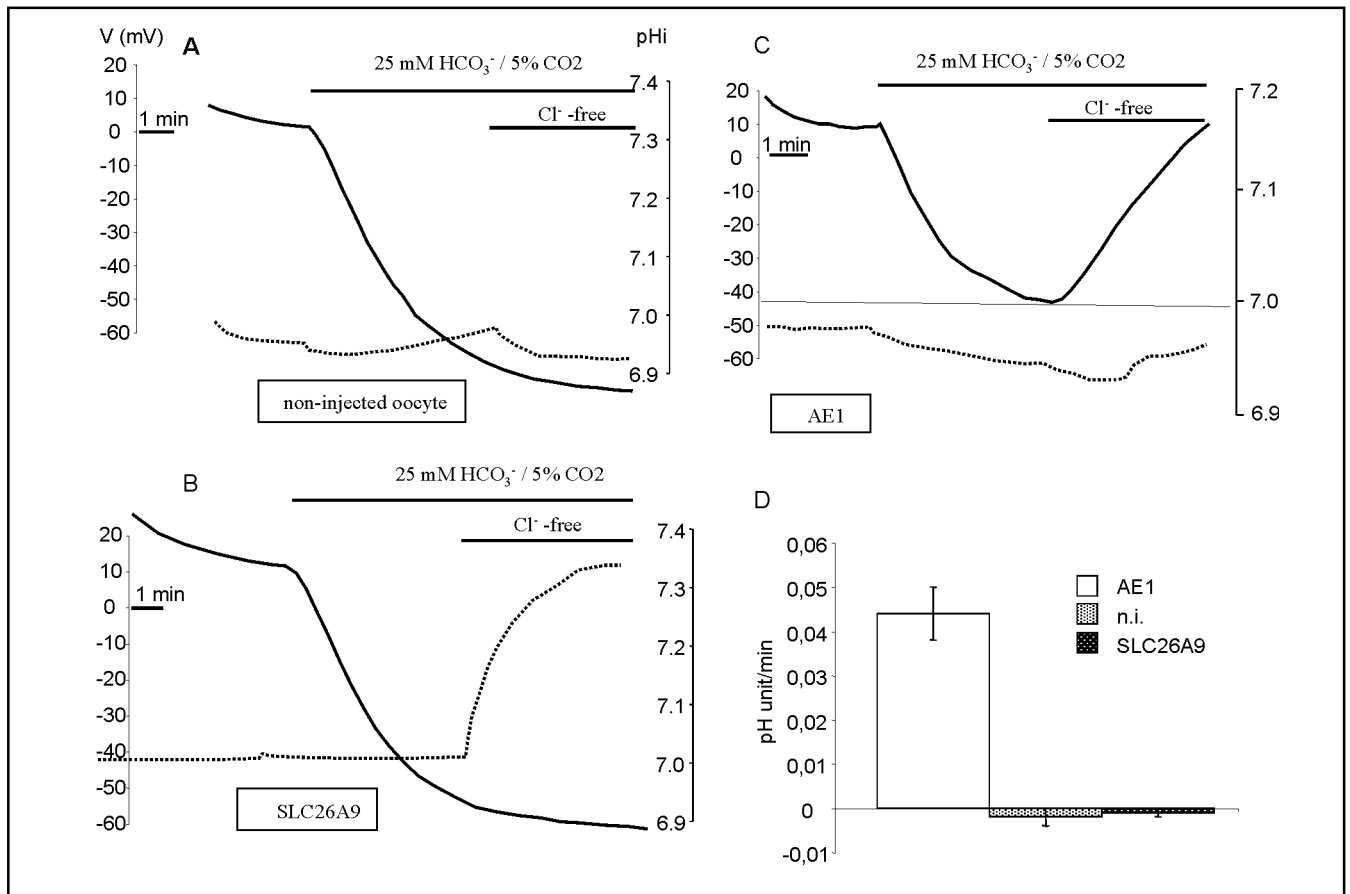


Fig. 7. SLC26A9 is not a Cl⁻/HCO₃⁻ exchanger. Illustrative experiments of changes in intracellular pH in non-injected oocytes (A) in SLC26A9 RNA-injected oocytes (B) and in AE1 RNA-injected oocytes (C). Oocytes are acidified in the presence of HCO₃⁻/CO₂. A subsequent change into a Cl⁻-free medium (Na-gluconate) allows the function of the Cl⁻/HCO₃⁻ exchanger AE1 and pH recovery. No pH recovery is observed in SLC26A9 RNA-injected oocytes or controls (n.i.). Voltage changes (mV) are indicated by dashed lines (D) Mean ± ES of the initial rates of pHi recovery (pH unit/min) in a Cl⁻-free medium.

(MBS) to a Kgluconate medium depolarizes the oocyte membrane potential of SLC26A9 cRNA-injected oocytes from -35.5 ± 0.9 mV to $+7.1 \pm 4.0$ mV, $n=10$. Oocytes were then clamped to the depolarizing potential throughout the entire experiment. Addition of 10 mM Cl⁻ to the Kgluconate medium induces the development of a clamping current in SLC26A9 cRNA-injected oocytes corresponding to Cl⁻ entry into these oocytes (Fig. 5). The addition of 10 mM HCO₃⁻ induces an 8 X lower increase in the clamping current compared to that observed with 10 mM Cl⁻, indicating that SLC26A9 presents a poor HCO₃⁻ conductivity. While non injected-oocytes perfused from MBS to a Kgluconate medium also depolarize (from -41.8 ± 2 mV to -13.9 ± 4 mV, $n=8$), minor changes in the clamping currents are observed in NI-oocytes submitted to the same experimental protocol (Cl⁻ or HCO₃⁻ addition).

A complementary approach was designed to detect the possible functioning of SLC26A9 as an electrogenic Cl⁻/HCO₃⁻ exchange. To this aim, we followed the clamping currents associated with the Cl⁻ efflux which develop when the perfusion solution is switched from MBS to a Cl⁻ free MBS (Cl⁻ was substituted by gluconate), anticipating that the presence of HCO₃⁻ would favor Cl⁻ efflux. This maneuver was either performed in the presence of 2.4 mM HCO₃⁻ (MBS, HEPES pH7.4) or with a higher HCO₃⁻ concentration (24 mM, gazing with 5% CO₂, pH 7.4). As illustrated in Fig. 7A, in presence of low [HCO₃⁻], switching the perfusing solution from a Cl⁻-containing medium (MBS) to a gluconate-containing medium induces the development of a clamping current (associated with the depolarization due to Cl⁻ exit from oocytes). The same protocol was then repeated in the presence of high HCO₃⁻/CO₂ concentrations.

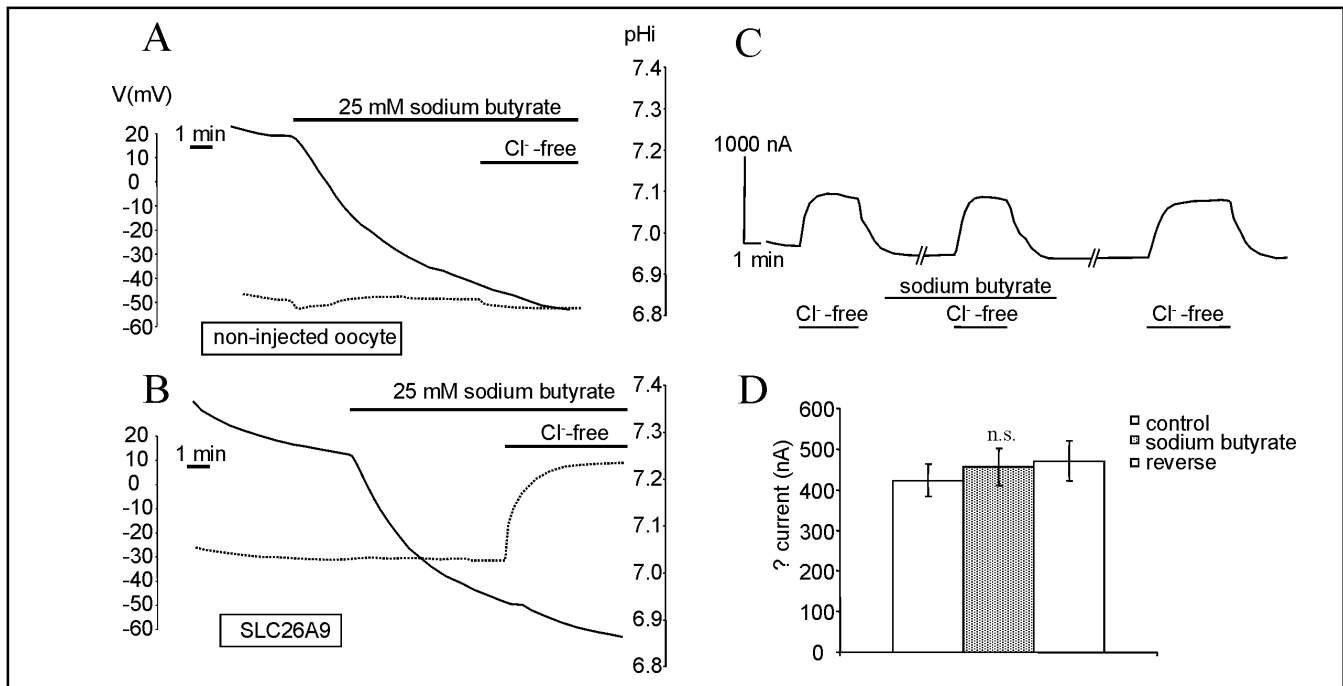


Fig. 8. Currents associated with SCL26A9 expression in *Xenopus laevis* oocytes are not affected by an intracellular acidification. Sodium butyrate (25 mM) application acidifies non-injected oocytes (A) and SLC26A9 cARN-injected oocytes (B). Voltage changes (mV) are indicated by dashed lines (C). Illustrative experiment of the clamping currents measured when the medium perfusing the SLC26A9 cRNA-injected oocyte is changed from MBS to a Cl⁻-free medium (Na-gluconate) in the absence or presence of Na-butyrate (25 mM). (D) Mean \pm ES of the clamping currents, $n = 9$, N.S.

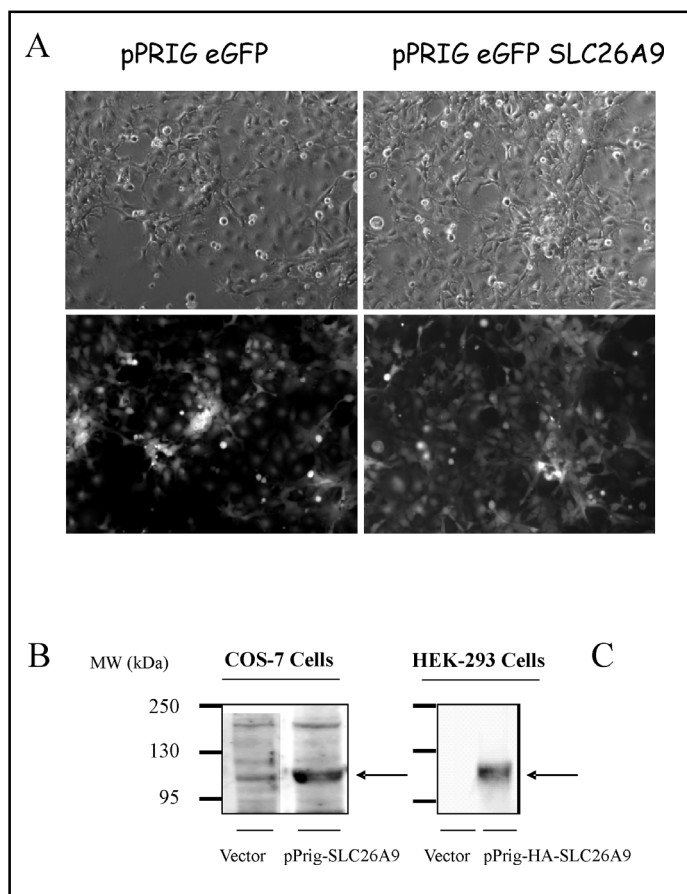
The presence of HCO_3^-/CO_2 in the perfusing solution has no significant effect on the resting current, confirming the low membrane permeability of SLC26A9 cRNA-injected oocytes to HCO_3^- (difference in clamping currents after HCO_3^-/CO_2 application is -42 ± 36 nA, $n=13$, n.s.). As expected, subsequent Cl⁻ substitution by gluconate still induces the development of a clamping current associated with Cl⁻ exit from the oocytes (Fig. 6A). However, the amplitude of the current is $41.9\% \pm 7.5$ larger ($p < 0.001$, $n=12$) than that measured in presence of low HCO_3^- concentrations (Fig. 6). Control of this effect by returning to low HCO_3^- concentrations reduces the amplitude of the currents, which develop by substitution of Cl⁻ to gluconate (Fig. 6A, last peak and Fig. 6B). Therefore the presence of HCO_3^-/CO_2 is found to favor Cl⁻ transport through membranes of SLC26A9 cRNA-injected oocytes, a finding which would be consistent with the functioning of an electrogenic Cl⁻/HCO₃⁻ exchanger.

SLC26A9 does not exchange HCO₃⁻ with Cl⁻

We directly measured the intracellular pH (pH_i) of SLC26A9 cRNA-injected oocytes using pH sensitive microelectrodes in conditions known to favor the Cl⁻/

HCO₃⁻ exchange. For these experiments, oocytes were first perfused with a HCO_3^-/CO_2 -containing medium. The perfusing medium was then replaced by a Cl⁻-free medium (still containing HCO_3^-/CO_2) to favor the functioning of the Cl⁻/HCO₃⁻ exchange (Cl⁻ efflux against HCO₃⁻ influx). Illustrative experiments are given in Fig. 7. As expected for a rapid CO₂ diffusion, oocytes acidify when passed from MBS to a HCO_3^-/CO_2 containing medium. This effect is pronounced in both non-injected oocytes (within 10 min pH_i switched from 7.22 ± 0.01 to 6.69 ± 0.04 , $n=6$, Fig. 7A) and in SLC26A9 cRNA-injected oocytes (within 10 min pH_i changes from 7.35 ± 0.01 to 6.93 ± 0.03 , $n=10$; Fig. 7B). While less marked, an oocyte acidification is also observed using AE1 cRNA-injected oocytes as a positive control for Cl⁻/HCO₃⁻ exchange activity (pH_i changes from 7.16 ± 0.02 to 6.93 ± 0.06 , $n=8$, Fig. 7C). AE1 cRNA-injected oocytes recovered their pH_i when Cl⁻ is substituted by gluconate as a consequence of a favorable driving forces for Cl⁻/HCO₃⁻ exchange. In contrast, both non-injected oocytes and SLC26A9 cRNA-injected oocytes are unable to recover their pH_i after such an anion substitution (Fig. 7A and 7B). This last finding indicates that SLC26A9 cannot

Fig. 9. COS-7 cell transduction with SLC26A9. (A) COS-7 cells transduced with pPRIG-eGFP or pPRIG-eGFP-SLC26A9 are visualized 24 h after transduction. The same field of cells photographed under visible light (upper panels) and UV fluorescence (lower panels) for pPRIG-eGFP (left) or pPRIG-eGFP-SLC26A9 (right) at 20 X magnification. (B) Immunoblot of lysates obtained from microsomal membranes following establishment of COS-7 pPRIG-eGFP (vector) or COS-7 pPRIG-eGFP-SLC26A9 (pPRIG-SLC26A9) cell populations. One band (arrow) migrating at about 105 kDa is observed in pPRIG-eGFP-SLC26A9 transduced cells which corresponds to the predicted size of SLC26A9 in mammalian cells. (C) A band migrating at the same apparent molecular weight is also observed in lysates from HEK-293 cells transfected with pPRIG-eGFP-HA-SLC26A9 and revealed with an anti-HA antibody (no bands are revealed in pPRIG-eGFP transfected HEK-293 cells, left). Molecular weight protein markers in kDa are indicated.



function as a $\text{Cl}^-/\text{HCO}_3^-$ exchanger under these experimental conditions. The mean rate \pm ES of pH_i recovery per minute, for the three different experimental groups, is given in Fig. 7D. As mentioned above, large changes in the membrane potential are observed in SLC26A9 RNA-injected oocytes upon substitution of gluconate for Cl^- , reflecting the Cl^- conductance through SLC26A9 (dashed lines of Fig. 7B).

Does an intracellular acidification stimulate SLC26A9 activity ?

From these experiments we concluded that the increase in Cl^- transport activity (Cl^- efflux) observed in the presence of $\text{HCO}_3^-/\text{CO}_2$ (see Fig. 6) is not associated with an HCO_3^- exchange (HCO_3^- entry) through SLC26A9. Since oocytes were acidified upon the application of $\text{HCO}_3^-/\text{CO}_2$, we tested a possible direct role of intracellular pH on the SLC26A9 activity. For this purpose, the weak acid, Na-butyrate (24 mM) was added to the perfusing MBS medium in order to induce a cell acidification. As expected, intracellular pH acidifies when Na-butyrate is added to the perfusing solution (Fig. 8A, 8B). This acidification is observed in non-injected oocytes (pH_i switched from 7.22 ± 0.01 to 6.81 ± 0.01 , $n=3$) as in

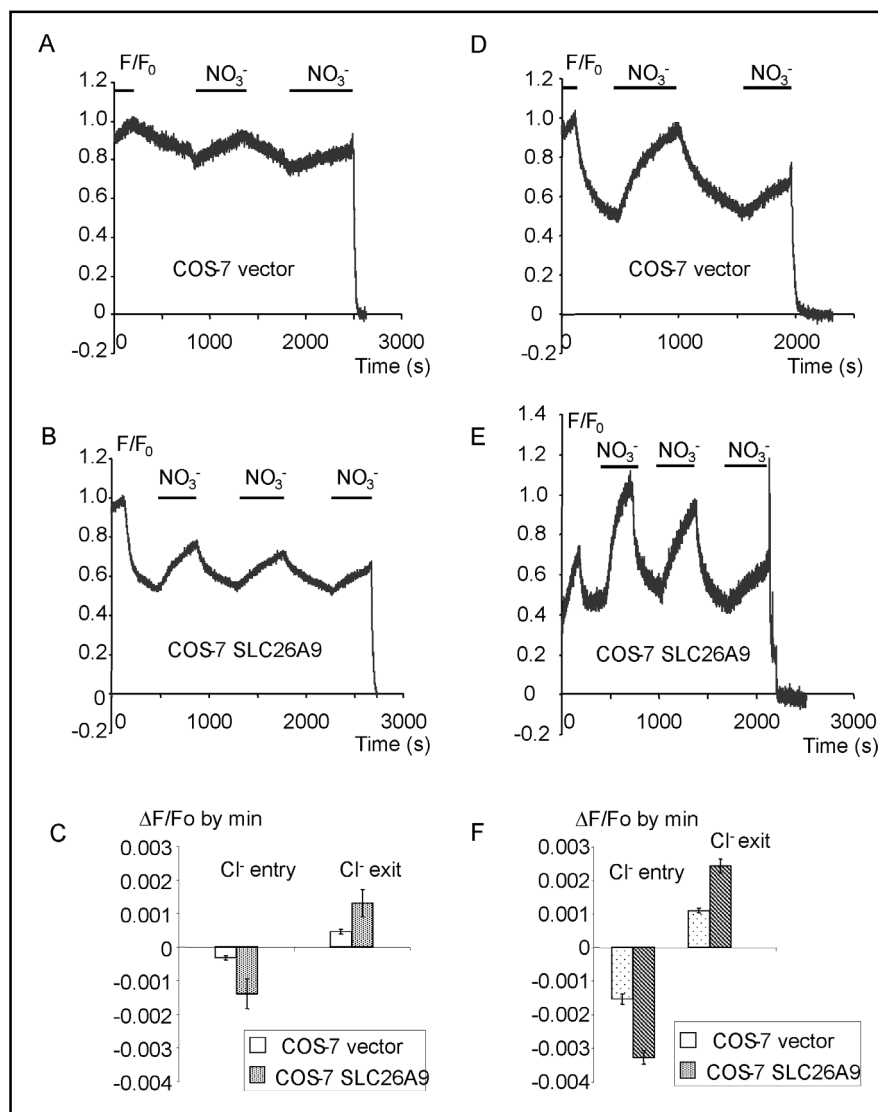
SLC26A9 cRNA-injected oocytes (pH_i switched from 7.27 ± 0.07 to 7.01 ± 0.03 , $n=5$) after 8 min of the weak acid application. Oocytes do not reverse their pH_i (alkalinize) when they are bathed in a Cl^- -free-solution but keep on acidifying in the presence of Nabutyrate.

A similar protocol was used to investigate the effect of an intracellular acidification induced by Nabutyrate, on the current generated by the Cl^- -substitution of MBS. Voltage clamp experiments indicate that the Cl^- -transporting activity of oocytes expressing SLC26A9 (Fig. 8C, 8D) is not affected by intracellular pH changes following Nabutyrate application.

SLC26A9 expression in a mammalian cell line

In order to validate and extend our observations obtained using the *Xenopus laevis* oocytes expression system, we expressed SLC26A9 in the COS-7 mammalian cell line. For this purpose, we generated two mixed populations of COS-7 cell lines by retroviral transduction using either the empty pPRIG-eGFP vector [26] or the pPRIG-eGFP-SLC26A9 vector. The efficiency of cell transduction was verified by following eGFP fluorescence expression. Over 95 % of the cells for both cell types were fluorescent (Fig. 9A), indicating

Fig. 10. Cl^- permeability is increased in COS-7 cells transduced with SLC26A9. Representative traces of the F/F_0 changes following Cl^- to NO_3^- substitution as a function of time in COS-7 cells transduced with pPRIG-eGFP (COS-7 vector; A) or (B) with pPRIG-eGFP-SLC26A9. The Ringer solution used was buffered with HEPES (10 mM). (C) Mean \pm ES of F/F_0 changes. $N=10$, $**p<0.001$. Representative traces of the F/F_0 changes following Cl^- to NO_3^- substitution in a Ringer solution containing 24 mM HCO_3^- and gazed with 5% CO_2 , pH 7.4 in COS-7 cells transduced with pPRIG-eGFP (COS-7 vector; D) or with pPRIG-eGFP-SLC26A9 (E). (F) Mean \pm ES of F/F_0 changes. $N=9$, $***p<0.001$.



that the cells were efficiently transduced and the expression of SLC26A9 was controlled by Western blot. A protein migrating around 105 kDa is detected in COS-7 cells transduced with pPRIG-eGFP-SLC26A9 whereas the same size protein corresponding to the endogenous SLC26A9 is weakly detected in lysates from pPRIG-eGFP transduced cells (Fig. 9B). Other weaker bands seen on the Western blot are non-specific. The HA-tagged SLC26A9 protein, transfected in HEK-293 cells and detected with an anti-HA antibody, migrates at a similar size as the SLC26A9 protein detected in pPRIG-eGFP-SLC26A9 transduced COS-7 cells (Fig. 9C). It should be noted that SLC26A9 migrates at a higher apparent molecular weight (105 kDa) than in *Xenopus* oocytes (around 85 kDa). This discrepancy is most likely due to a difference in the glycosylation of the protein in both expression systems.

The functionality of SLC26A9 in transduced COS-7 cells was verified by following the kinetic parameters of Cl_i^- changes when Cl^- in the Ringer solution was substituted by NO_3^- , an experiment giving an index of the membrane Cl^- permeability. Cl^- permeability of pPRIG-eGFP transduced cells (control) is low in a HCO_3^- -free Ringer solution (Fig. 10A) but is increased 3 to 4 X in pPRIG-eGFP-SLC26A9 transduced cells (Fig. 10B and 10C), indicating the functionality of SLC26A9.

When cells are perfused with a $\text{HCO}_3^-/\text{CO}_2$ containing Ringer, Cl^- permeability of control cells is increased in comparison to that measured in a HCO_3^- -free Ringer solution (compare Fig. 10A and Fig. 10D). This finding is indicative of the development of a $\text{HCO}_3^-/\text{CO}_2$ -sensitive Cl^- transporting pathway, probably mediated by an endogenous $\text{Cl}^-/\text{HCO}_3^-$ exchanger in COS-7 cells. Nevertheless, pPRIG-eGFP-SLC26A9

transduced cells exhibit a nearly twice larger Cl^- permeability in presence of $\text{HCO}_3^-/\text{CO}_2$ (Fig. 10E) than that observed with control cells (Fig. 10D and 10F). Assuming a constant endogenous $\text{Cl}^-/\text{HCO}_3^-$ exchanger activity, the Cl^- transport through SLC26A9 would correspond to the difference between Cl^- changes in pPRIG-eGFP-SLC26A9 transduced cells and control cells. With this assumption, Cl^- influx rates associated with SLC26A9 expression are increased 2.1 X ($p < 0.01$, $n = 8$) and Cl^- effluxes rates are increased 1.9 X ($p < 0.05$, $n = 8$) in a $\text{HCO}_3^-/\text{CO}_2$ containing medium as compared to Cl^- transport rates obtained in a $\text{HCO}_3^-/\text{CO}_2$ free medium. Therefore, the presence of $\text{HCO}_3^-/\text{CO}_2$ stimulates the Cl^- permeability of SLC26A9 transduced cells.

We then tested the possibility that SLC26A9 functions as an anion exchanger in COS-7 cells, a property that we did not find in *Xenopus laevis* oocytes (see above). pH_i changes of COS-7 cells are therefore followed using BCECF as an intracellular pH probe. As illustrated by Fig. 11A and 11B, changing the Cl^- -containing HEPES medium to a $\text{HCO}_3^-/\text{CO}_2$ containing medium acidifies the cells. Subsequent perfusion of the cells with a Cl^- -free HEPES solution (to stimulate Cl^- efflux and eventual associated HCO_3^- influx) induces a slight pH_i increase. However, similar pH changes (Fig. 11C) are observed in both pPRIG-eGFP and pPRIG-eGFP-SLC26A9 transduced cells, suggesting that we are dealing with the activity of an endogenous anion transporter in both transduced cell types. Therefore no specific $\text{Cl}^-/\text{HCO}_3^-$ exchange is associated with SLC26A9 activity in either COS-7 mammalian cells or *Xenopus laevis* oocytes protein expression systems.

Discussion

In the present work, using two different systems of protein expression, *Xenopus laevis* oocytes and COS-7 cells, we present evidence that SLC26A9 behaves as an anion channel and not as an anion transporter exchanging Cl^- against HCO_3^- . Indeed, the HCO_3^- permeability through SLC26A9 is low but we demonstrated that the presence of HCO_3^- , by itself was found to exert a positive control on the Cl^- transport. In addition, calcium was found to negatively modulate SLC26A9 activity.

Distinguishing between the transporting properties of an anion channel from those of an electrogenic anion exchanger is not easy and conclusions may be controversial. For example, CIC-5 and CIC-4 were initially

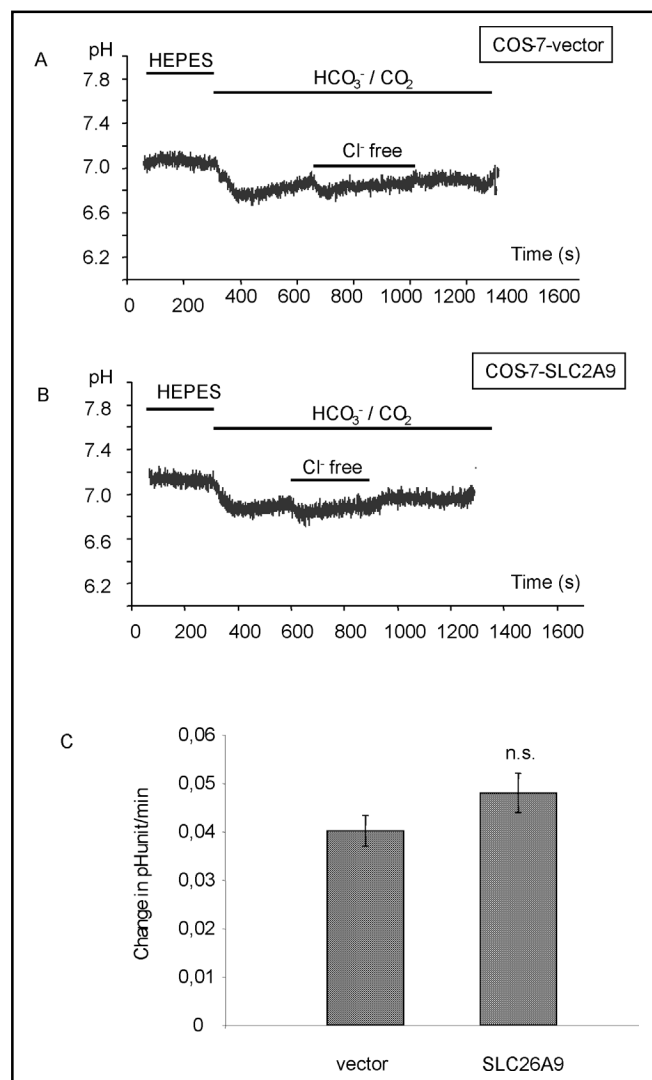


Fig. 11. SLC26A9 does not mediate a $\text{Cl}^-/\text{HCO}_3^-$ exchange in pPRIG-eGFP-SLC26A9 transduced cells. (A) Intracellular pH changes following $\text{HCO}_3^-/\text{CO}_2$ containing Ringer and subsequent Cl^- free-Ringer application in pPRIG-eGFP COS-7 (COS-7 vector). (B) same protocol with COS-7 cells transduced with pPRIG-eGFP-SLC26A9. (C) Initial rates of pH recovery (Mean \pm ES expressed as pH unit/min, $n=6$) of both batches of COS-7 cells when the Ringer solution is changed to a Cl^- -free Ringer solution.

described as anion channels [34-36] but were later described as anion antiporters [37]. AE1, a typical anion exchanger, was surprisingly found to develop a conductive pathway in one mutated form [38]. SLC26A7 which was initially described as an anion exchanger [10] was later characterized as a Cl^- channel [14].

We found that SLC26A9 RNA-injected *Xenopus laevis* oocytes developed anion currents, a common property between a channel and an electrogenic

transporter; the anion selectivity calculated by the P_x/P_{Cl} ratio was $I^- > NO_3^- > Cl^- > \text{gluconate} > SO_4^{2-}$ and the sequence of currents measured at +80 mV (outward current) was of $Cl^- > I^- > NO_3^- \geq \text{gluconate} > SO_4^{2-}$. Cl^- currents generated by increasing the medium concentration of Cl^- obey a linear relationship in the tested range (0–80 mM), which differs from Michaelis-Menten relationships usually given for one of the characteristic of an anion carrier (see [39] for AE1). HCO_3^- was poorly transported in *Xenopus laevis* oocytes expressing SLC26A9. Indeed, currents of very low amplitudes were generated by HCO_3^- application in comparison to those observed with similar Cl^- concentrations. Furthermore, HCO_3^- was not exchanged against Cl^- as revealed by the absence of pH_i changes in conditions expected to favor a Cl^-/HCO_3^- exchange mechanism. In SLC26A9 transduced COS-7 cells, our attempts to reveal the presence of a Cl^-/HCO_3^- exchange associated with SLC26A9 expression also failed. These cells presented a significant increase of their membrane anion permeability, indicative of functional SLC26A9, but we were unable to reveal an associated HCO_3^- transport (by pH_i changes) in conditions favorable to a Cl^-/HCO_3^- exchange.

Among the tested anion blockers, NS 3623 at a relatively high concentration of 500 μM was the most effective on oocyte currents associated with SLC26A9 expression. NS 3623 gave a 49% inhibition of the currents while DIDS, already described as a modest inhibitor of SLC26A9 [12] inhibited the currents by 38 %. NS 3623 have previously been reported to block a Cl^- conductance in mouse erythrocytes [31] and to inhibit the endogenous volume regulated anion channel in HEK293 cells [40]. The specific CFTR inhibitor (CFTR(inh)-172) had a very small effect at the low concentration used of 2 μM (or 5 μM , data not shown), a dose known to inhibit CFTR in airways [41] and in CFTR cRNA-injected oocytes (present study).

Taking into account these different findings, SLC26A9 does not function as an electrogenic anion exchanger. However, our experiments indicate that SLC26A9 functions as an anion channel with a preferential Cl^- permeability. This conclusion is similar to that found by Dorwart *et al.* 2007 (see review [12]) and to our preliminary data using *Xenopus laevis* oocytes [42] even though SLC26A9 was initially thought to be an anion transporter [11]. An electrogenic anion transporter with a nCl^-/pA^- stoichiometry (with $n \gg p$) cannot be totally excluded.

We found that the presence of HCO_3^-/CO_2 in the

oocyte perfusing medium activated Cl^- currents in SLC26A9-cRNA-injected oocytes. This effect cannot be attributed to a condition favoring a Cl^-/HCO_3^- exchange since HCO_3^- was not exchanged by Cl^- . It is also unlikely that oocyte acidification by cell CO_2 diffusion which was observed in our pH_i measurements experiments, was at the origin of this stimulation. Indeed, Nabutyrate application which induced a similar acidification, did not stimulate the Cl^- currents associated with SLC26A9 expression. Therefore, an acidic pH has no effect (in the tested range) on SLC26A9 activity. In addition, we also found in SLC26A9 transduced COS-7 cells in presence of HCO_3^-/CO_2 that the rates of Cl^- transport (influx and efflux) of these cells were larger than those measured in HCO_3^-/CO_2 -free media. A possibility which would account for our results in *Xenopus laevis*-and COS-7 cells-expression systems would be that HCO_3^- directly modulates the gating state of the channel. Such a proposal has already been given for prestin (SLC26A5), the outer hair cell motor protein, for which Cl^- and HCO_3^- intracellular anions act as extrinsic voltage sensors [43, 44]. These authors proposed that after binding to a site with millimolar affinity, these anions are translocated across the membrane by the transmembrane voltage triggering conformational changes of the protein. Gating properties (inhibitory effect) of I^- , Br^- and polyatomic anions (SCN^- , NO_3^- , $CH_3SO_3^-$) have also been reported for hCIC-1, a voltage-gated Cl^- channel (or antiporter) of the CIC-family [45, 46]. The inhibitory effect of NO_3^- and I^- on Cl^- transport mediated by SLC26A9 that we report here would be consistent with such a channel gating mechanism by anions. Nevertheless, our proposal that HCO_3^- could be a direct modulator of the gating state of the SLC26A9 channel would require further studies at the channel level using patch-clamp experiments.

We found that large intracellular calcium increases had inhibitory effects on the anionic currents associated with SLC26A9 activity. This effect was found with thapsigargin (in presence or absence of extracellular calcium) since this agent is known to release calcium from intracellular stores. Ionomycin had a similar effect, even in a calcium-free media since ionomycin was found to also increase the release from intracellular stores in addition to its well known effect on the plasma membrane permeability [32]. The down regulation of currents through SLC26A9 by large intracellular calcium concentrations could be associated with smaller and more physiological calcium changes involved in a signaling pathway.

Retroviral transduction, or viral-mediated transfer of DNA into cells, is delivery option that offers the most

efficient means of gene delivery to a wide variety of dividing cells. Indeed, 24h after transduction we observed that over 95% of all COS-7 cells were GFP-positive, thus efficiently transduced. Another major advantage for using retroviruses is that the expression of the protein of interest remains at physiological levels especially when compared to transient transfections where the same protein is highly overexpressed which could lead to aberrant results. Finally, integrations into the host genome are random thus reducing the possibility of aberrant effects on gene expression. Thus, the establishment of a mixed population of COS-7 cells constitutively expressing SLC26A9 will continue to remain a useful tool for future studies in elucidating SLC26A9 function.

SLC26A9 was initially identified in lung [10] and gastric epithelia [11]. For this reason we cloned SLC26A9 from primary human bronchial cells culture (NHBE). We also identified SLC26A9 at the RNA level in two human bronchial cell lines, 16HBE14o- and in CFBE41o-, a cell line derived from cystic fibrosis bronchial cells (unpublished results). The role of SLC26A9 remains to be determined in bronchial tissue since this channel may

participate to the transepithelial anion transport. A significant and direct role in the maintenance of the pH of the airway surface liquid is unlikely since SLC26A9 is poorly permeable to HCO_3^- and therefore differs in that respect to other members of the SLC26 family [1, 2]. However, although CFTR is the main Cl^- channel involved in the transepithelial chloride secretion, SLC26A9 could participate in this secretion and could represent an alternative CFTR Cl^- channel.

Acknowledgements

This study was supported by CNRS, UNSA and the CF association (VLM). We thanks Dr. H. Guizouarn for helpful discussion and P. Martin for providing retroviral vectors. We also thanks M.V. Guillot-Sestier for performing preliminary experiments. While this manuscript was in preparation, a paper by Muallem's laboratory (Dorwart *et al.*, 2007, see review [12]) was published also proposing that SLC26A9 is functioning as an anion channel.

References

- Mount DB, Romero MF: The SLC26 gene family of multifunctional anion exchangers. *Pflugers Arch* 2004;447:710-21.
- Ko SB, Zeng W, Dorwart MR, Luo X, Kim KH, Millen L, Goto H, Naruse S, Soyombo A, Thomas PJ, Muallem S: Gating of CFTR by the STAS domain of SLC26 transporters. *Nat Cell Biol* 2004;4:343-50.
- Melvin JE, Park K, Richardson L, Schultheis PJ, Shull GE: Mouse down-regulated in adenoma (DRA) is an intestinal $\text{Cl}^-/\text{HCO}_3^-$ exchanger and is up-regulated in colon of mice lacking the NHE3 Na^+/H^+ exchanger. *J Biol Chem* 1999;274:22855-61.
- Jacob P, Rossmann H, Lamprecht G, Kretz A, Neff C, Lin-Wu E, Gregor M, Groneberg DA, Kere J, Seidler U: Down-regulated in adenoma mediates apical $\text{Cl}^-/\text{HCO}_3^-$ exchange in rabbit, rat, and human duodenum. *Gastroenterology* 2002;122:709-24.
- Soleimani M, Greeley T, Petrovic S, Wang Z, Amlal H, Kopp P, Burnham CE: Pendrin: an apical $\text{Cl}^-/\text{OH}^-/\text{HCO}_3^-$ exchanger in the kidney cortex. *Am J Physiol Renal Physiol* 2001;280:F356-64.
- Scott DA, Wang R, Kremann TM, Sheffield VC, Karniski LP, Ko SB, Zeng W, Dorwart MR, Luo X, Kim KH, Millen L, Goto H, Naruse S, Soyombo A, Thomas PJ, Muallem S: The Pendred syndrome gene encodes a chloride-iodide transport protein. *Nat Genet* 1999;21:440-3.
- Everett LA, Glaser B, Beck JC, Idol JR, Buchs A, Heyman M, Adawi F, Hazani E, Nassir E, Baxevas AD, Sheffield VC, Green ED: Pendred syndrome is caused by mutations in a putative sulphate transporter gene (PDS). *Nat Genet* 1997;17:411-22.
- Royaux IE, Wall SM, Karniski LP, Everett LA, Suzuki K, Knepper MA, Green ED: Pendrin, encoded by the Pendred syndrome gene, resides in the apical region of renal intercalated cells and mediates bicarbonate secretion. *Proc Natl Acad Sci U S A* 2001;98:4221-6.
- Wang Z, Petrovic S, Mann E, Soleimani M: Identification of an apical $\text{Cl}^-/\text{HCO}_3^-$ exchanger in the small intestine. *Am J Physiol Gastrointest Liver Physiol* 2002;282:G573-9.
- Lohi H, Kujala M, Makela S, Lehtonen E, Kestila M, Saarialho-Kere U, Markovich D, Kere J: Functional characterization of three novel tissue-specific anion exchangers SLC26A7, -A8, and -A9. *J Biol Chem* 2002;277:14246-54.
- Xu J, Henriksnas J, Barone S, Witte D, Shull GE, Forte JG, Holm L, Soleimani M: SLC26A9 is expressed in gastric surface epithelial cells, mediates $\text{Cl}^-/\text{HCO}_3^-$ exchange, and is inhibited by NH_4^+ . *Am J Physiol Cell Physiol* 2005;289:C493-505.
- Dorwart MR, Shcheynikov N, Wang Y, Stippec S, Muallem S: SLC26A9 is a Cl^- channel regulated by the WNK kinases. *J Physiol* 2007;584:333-45.
- Barone S, Amlal H, Xu J, Kujala M, Kere J, Petrovic S, Soleimani M: Differential regulation of basolateral $\text{Cl}^-/\text{HCO}_3^-$ exchangers SLC26A7 and AE1 in kidney outer medullary collecting duct. *J Am Soc Nephrol* 2004;15:2002-11.
- Kim KH, Shcheynikov N, Wang Y, Muallem S: SLC26A7 is a Cl^- channel regulated by intracellular pH. *J Biol Chem* 2005;280:6463-70.

- 15 Gabriel SE, Clarke LL, Boucher RC, Stutts MJ: CFTR and outward rectifying chloride channels are distinct proteins with a regulatory relationship. *Nature* 1993;63(6426):263-8.
- 16 Schwiebert EM, Egan ME, Hwang TH, Fulmer SB, Allen SS, Cutting GR, Guggino WB: CFTR regulates outwardly rectifying chloride channels through an autocrine mechanism involving ATP. *Cell* 1995;81:1063-73.
- 17 Anderson MP, Welsh MJ: Calcium and cAMP activate different chloride channels in the apical membrane of normal and cystic fibrosis epithelia. *Proc Natl Acad Sci U S A* 1991;88:6003-7.
- 18 Clarke LL, Grubb BR, Yankaskas JR, Cotton CU, McKenzie A, Boucher RC: Relationship of a non-cystic fibrosis transmembrane conductance regulator-mediated chloride conductance to organ-level disease in Cftr(-/-) mice. *Proc Natl Acad Sci U S A* 1994;91:479-83.
- 19 Schwiebert EM, Flotte T, Cutting GR, Guggino WB: Both CFTR and outwardly rectifying chloride channels contribute to cAMP-stimulated whole cell chloride currents. *Am J Physiol* 1994;266:C1464-77.
- 20 Jovov B, Ismailov II, Berdiev BK, Fuller CM, Sorscher EJ, Dedman JR, Kaetzel MA, Benos DJ: Interaction between cystic fibrosis transmembrane conductance regulator and outwardly rectified chloride channels. *J Biol Chem* 1995;270:29194-200.
- 21 Schwiebert EM, Cid-Soto LP, Stafford D, Carter M, Blaisdell CJ, Zeitlin PL, Guggino WB, Cutting GR: Analysis of ClC-2 channels as an alternative pathway for chloride conduction in cystic fibrosis airway cells. *Proc Natl Acad Sci U S A* 1998;95:3879-84.
- 22 Wei L, Vankeerberghen A, Cuppens H, Eggermont J, Cassiman JJ, Droogmans G, Nilius B: Interaction between calcium-activated chloride channels and the cystic fibrosis transmembrane conductance regulator. *Pflügers Arch* 1999;438:635-41.
- 23 Wei L, Vankeerberghen A, Cuppens H, Cassiman JJ, Droogmans G, Nilius B: The C-terminal part of the R-domain, but not the PDZ binding motif, of CFTR is involved in interaction with Ca(2+)-activated Cl⁻ channels. *Pflügers Arch* 2001;442:280-5.
- 24 Kunzelmann K, Mall M, Briel M, Hipper A, Nitschke R, Ricken S, Greger R: The cystic fibrosis transmembrane conductance regulator attenuates the endogenous Ca²⁺ activated Cl⁻ conductance of *Xenopus laevis* oocytes. *Pflügers Arch* 1997;435:178-81.
- 25 Chomczynski P, Sacchi N: Single-step method of RNA isolation by acid guanidinium thiocyanate-phenol-chloroform extraction. *Anal Biochem* 1987;162:156-9.
- 26 Martin P, Albagli O, Poggi MC, Boulukos KE, Pognonec P: of a new bicistronic retroviral vector with strong IRES activity. *BMC Biotechnol. Development* 2006;12:6-4.
- 27 Ratcliff FG, Ehrenfeld J: Activation of osmotically-activated potassium transporters after injection of mRNA from A6 cells in *Xenopus laevis* oocytes. *Biochim Biophys Acta* 1994;1190:248-56.
- 28 Schmieder S, Lindenthal S, Banderali U, Ehrenfeld J: Characterization of the putative chloride channel xClC-5 expressed in *Xenopus laevis* oocytes and comparison with endogenous chloride currents. *J Physiol* 1998;511:379-93.
- 29 Guizouarn H, Martial S, Gabillat N, Borgese F: Point mutations involved in red cell stomatocytosis convert the electroneutral anion exchanger 1 to a nonselective cation conductance. *Blood* 2007;110:2158-65.
- 30 Brochiero E, Banderali U, Lindenthal S, Raschi C, Ehrenfeld J: Basolateral membrane chloride permeability of A6 cells: implication in cell volume regulation. *Pflügers Arch* 1995;431:32-45.
- 31 Bennekou P, de Franceschi L, Pedersen O, Lian L, Asakura T, Evans G, Brugnara C, Christophersen P: Treatment with NS3623, a novel Cl⁻conductance blocker, ameliorates erythrocyte dehydration in transgenic SAD mice: a possible new therapeutic approach for sickle cell disease. *Blood* 2001;97:1451-7.
- 32 Yoshida S, Plant S: Mechanism of release of Ca²⁺ from intracellular stores in response to ionomycin in oocytes of the frog *Xenopus laevis*. *J Physiol* 1992;458:307-18.
- 33 Lupu-Meiri M, Beit-Or A, Christensen SB, Oron Y: Calcium entry in *Xenopus* oocytes: effects of inositol trisphosphate, thapsigargin and DMSO. *Cell Calcium* 1993;14:101-10.
- 34 Steinmeyer K, Schwappach B, Bens M, Vandewalle A, Jentsch TJ: Cloning and functional expression of rat CLC-5, a chloride channel related to kidney disease. *J Biol Chem* 1995;270:31172-7.
- 35 Fisher SE, van Bakel I, Lloyd SE, Pearce SH, Thakker RV, Craig IW: Cloning and characterization of CLCN5, the human kidney chloride channel gene implicated in Dent disease (an X-linked hereditary nephrolithiasis). *Genomics* 1995;29:598-606.
- 36 Friedrich T, Breiderhoff T, Jentsch TJ: Mutational analysis demonstrates that ClC-4 and ClC-5 directly mediate plasma membrane currents. *J Biol Chem* 1999;274:896-902.
- 37 Picollo A, Pusch M: Chloride/proton antiporter activity of mammalian CLC proteins ClC-4 and ClC-5. *Nature* 2005;436:420-3.
- 38 Bruce LJ, Robinson HC, Guizouarn H, Borgese F, Harrison P, King MJ, Goede JS, Coles SE, Gore DM, Lutz HU, Ficarella R, Layton DM, Iolascon A, Ellory JC, Stewart GW: Monovalent cation leaks in human red cells caused by single amino-acid substitutions in the transport domain of the band 3 chloride-bicarbonate exchanger, AE1. *Nat Genet* 2005;11:1258-63.
- 39 Brahm J, Gasberg P, Funder J: kinetics of anion transport across the human red cell membrane. In *Progress in Cell Research*, 1992; Vol2 E. Bamberg and H. Passow (Eds) Elsevier Science Publishers B.V.
- 40 Stummann TC, Poulsen JH, Hay-Schmidt A, Grunnet M, Klaerke DA, Rasmussen HB, Olesen SP, Jorgensen NK: Pharmacological investigation of the role of ion channels in salivary secretion. *Pflügers Arch* 2003;446:78-87.
- 41 Thiagarajah JR, Song Y, Haggie PM, Verkman AS: A small molecule CFTR inhibitor produces cystic fibrosis-like submucosal gland fluid secretions in normal airways. *FASEB J* 2004;18:875-7.
- 42 Dulong S, Guillot-Sestier MV, Gabillat N, Borgese F, Ehrenfeld J: Functional characterization of SLC26A9, an anionic transporter in airway epithelia. *Rev Mal Respir. Abstracts of the Meeting of Respiratory Research (J2R)*, Tours, France, 13-14 October 2006;23:507 91.
- 43 Oliver D, He DZ, Klocker N, Ludwig J, Schulte U, Waldegger S, Ruppersberg JP, Dallos P, Fakler B: Intracellular anions as the voltage sensor of prestin, the outer hair cell motor protein. *Science* 2001;292:2340-3.
- 44 Oliver D, Schächinger T, Fakler B: Interaction of prestin (SLC26A5) with monovalent intracellular anions. *Novartis Found Symp* 2006;273:244-53;discussion 253-60, 261-4.
- 45 Fahlke C, Beck CL, George AL Jr: A mutation in autosomal dominant myotonia congenita affects pore properties of the muscle chloride channel. *Proc Natl Acad Sci U S A* 1997;94:2729-34.
- 46 Fahlke C, Yu HT, Beck CL, Rhodes TH, George AL Jr: Pore-forming segments in voltage-gated chloride channels. *Nature* 1997;390:529-32.